

Spatial and Temporal Variability of Benthic Respiration in a Scottish Sea Loch Impacted by Fish Farming: A Combination of In Situ Techniques

Cécile Cathalot, Bruno Lansard, Per O. J. Hall, Anders Tengberg, Elin Almroth-Rosell, Anna Apler, Lois Calder, Elanor Bell, et al.

Aquatic Geochemistry

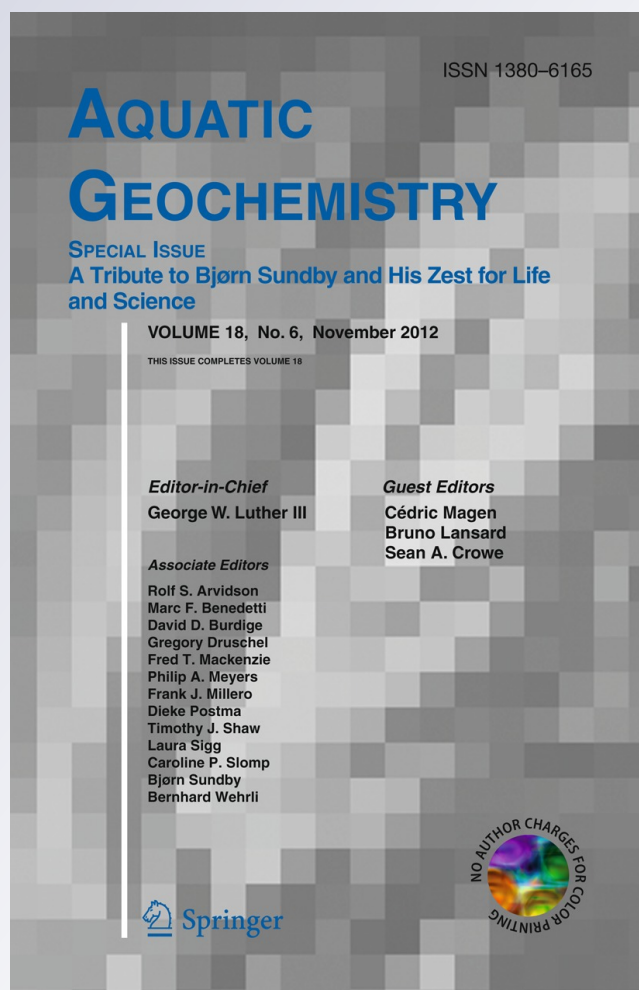
ISSN 1380-6165

Volume 18

Number 6

Aquat Geochem (2012) 18:515-541

DOI 10.1007/s10498-012-9181-4



Your article is protected by copyright and all rights are held exclusively by Springer Science +Business Media Dordrecht. This e-offprint is for personal use only and shall not be self-archived in electronic repositories. If you wish to self-archive your work, please use the accepted author's version for posting to your own website or your institution's repository. You may further deposit the accepted author's version on a funder's repository at a funder's request, provided it is not made publicly available until 12 months after publication.

Spatial and Temporal Variability of Benthic Respiration in a Scottish Sea Loch Impacted by Fish Farming: A Combination of In Situ Techniques

Cécile Cathalot · Bruno Lansard · Per O. J. Hall · Anders Tengberg · Elin Almroth-Rosell · Anna Apler · Lois Calder · Elanor Bell · Christophe Rabouille

Received: 15 March 2012 / Accepted: 13 October 2012 / Published online: 7 November 2012
© Springer Science+Business Media Dordrecht 2012

Abstract The effects of fish farm activities on sediment biogeochemistry were investigated in Loch Creran (Western Scotland) from March to October 2006. Sediment oxygen uptake rates (SOU) were estimated along an organic matter gradient generated from an Atlantic salmon farm using a combination of in situ techniques: microelectrodes, planar optode and benthic chamber incubations. Sulphide (H_2S) and pH distributions in sediment porewater were also measured using in situ microelectrodes, and dissolved inorganic carbon (DIC) fluxes were measured in situ using benthic chambers. Relationships between benthic fluxes, vertical distribution of oxidants and reduced compounds in the sediment were examined as well as bacterial abundance and biomass. Seasonal variations in SOU were relatively low and mainly driven by seasonal temperature variations. The effect of the fish farm on sediment oxygen uptake rate was clearly identified by higher total and diffusive oxygen uptake rates (TOU and DOU, respectively) on impacted stations (TOU: $70 \pm 25 \text{ mmol O}_2 \text{ m}^{-2} \text{ day}^{-1}$; DOU: $70 \pm 32 \text{ mmol O}_2 \text{ m}^{-2} \text{ day}^{-1}$ recalculated at the summer temperature), compared with the reference station (TOU: $28.3 \pm 5.5 \text{ mmol O}_2 \text{ m}^{-2} \text{ day}^{-1}$; DOU: $21.5 \pm 4.5 \text{ mmol O}_2 \text{ m}^{-2} \text{ day}^{-1}$). At the impacted stations, planar

Special issue in honour of Pr Bjørn Sundby.

C. Cathalot · B. Lansard · C. Rabouille (✉)
Laboratoire des Sciences du Climat et de l'Environnement, CEA-CNRS-UVSQ and IPSL, UMR 8212,
Avenue de la Terrasse, 91198 Gif-sur-Yvette, France
e-mail: rabouill@lscce.ipsl.fr

P. O. J. Hall · A. Tengberg · E. Almroth-Rosell
Department of Chemistry and Molecular Biology, Marine Chemistry, University of Gothenburg,
412 96 Gothenburg, Sweden

A. Apler
Geological Survey of Sweden, Box 670, 751 28 Uppsala, Sweden

L. Calder · E. Bell
Scottish Association for Marine Science, Dunstaffnage Marine Laboratory, Oban, Argyll PA37 1QA,
Scotland, UK

optode images displayed high centimetre scale heterogeneity in oxygen distribution underlining the control of oxygen dynamics by small-scale processes. The organic carbon enrichment led to enhanced sulphate reduction as demonstrated by large vertical H_2S concentration gradients in the porewater (from 0 to 1,000 μM in the top 3 cm) at the most impacted site. The impact on ecosystem functions such as bioirrigation was evidenced by a decreasing TOU/DOU ratio, from 1.7 in the non-impacted sediments to 1 in the impacted zone. This trend was related to a shift in the macrofaunal assemblage and an increase in sediment bacterial population. The turnover time of the organic load of the sediment was estimated to be over 6 years.

Keywords Fish farming · Microprofiling · Oxygen · H_2S · Sediment · Benthic chamber · Sea loch · Scotland · Benthic mineralization · Organic carbon

1 Introduction

Scottish fish farms are the largest producers of Atlantic salmon (*Salmo salar*) in the EU, with more than 10^5 tons of salmon produced in 2006 (Scottish Fish Farms Annual Production Survey, 2006; FAO, 2006). Aquaculture is therefore an important contribution to the Scottish rural economy. Nevertheless, fish farming activities generate huge amount of labile organic matter in the form of uneaten fish food or fish faeces that accumulate in the sediment (Oconnor et al. 1989; Brooks 2001; Mulsow et al. 2006). Such organic enrichment can lead to severe sediment anoxia, impact sedimentation and trophic networks (Hargrave et al. 2008) and modify the functioning of the benthic coastal ecosystem located within the fish farm vicinity. Excess organic matter reaching the seafloor increases the sediment oxygen uptake rate, which integrates microbial respiration, chemical oxidation and infaunal metabolism (Canfield et al. 1993b; Valiela et al. 1992; Hansen and Kristensen 1997). The risks of hypoxic or anoxic events in the water column rise substantially with large organic enrichment: when delivered to the bottom waters, the sulphides produced by anoxic mineralization can exert a negative feedback worsening the anoxia (Chapelle et al. 2001; Rabouille et al. 2008). Organic matter enrichment and consequent hypoxic events are well known to significantly alter the redox chemistry of the solid and porewater phase in the sediment by modifying the distributions and concentrations of chemical oxidant and reduced species (Vaquer-Sunyer and Duarte 2010). These processes also affect biological and physical characteristics of the sediment. Effective actions for quality enhancement and management of coastal ecosystems must be underpinned by a sound ecological and geochemical understanding of benthic processes (Hall et al. 1990).

The aim of this study was to examine the impact of organic enrichment from a Scottish fish farm on benthic mineralization processes over both temporal and spatial scales (seasonal and kilometric scales, respectively). Organic matter recycling was determined by using a suite of different in situ techniques including microelectrode microprofiling, planar optode imaging and benthic chambers deployments. These combined measurements allowed the quantification of benthic O_2 and dissolved inorganic carbon (DIC) fluxes as well as the acquisition of highly resolved sediment distributions of O_2 , pH and H_2S . In this paper, we examine the heterogeneity of organic matter deposition in sediment located under a fish farm in Loch Creran, the recycling of the organic matter in disturbed and reference sediments, its consequence on sediment biogeochemistry and the response of the benthic ecosystem to the perturbation induced by the fish farm activities.

2 Materials and Methods

2.1 Study Site

This study was conducted in the second basin of Loch Creran: a semi-enclosed sea loch located on the Scottish west coast (Fig. 1). The loch is 12.8 km long and divided into four basins, each separated by a shallow sill. The basin studied in this paper has relatively low tides (around 2 m tidal heights) and mostly soft, muddy sediments (Nickell et al. 2003). The loch receives a freshwater input of $290 \times 10^6 \text{ m}^3 \text{ year}^{-1}$ and is well mixed due to wind and tidal effects. Flushing time in the entire loch is approximately 3 days, over which around 60 % of water volume is exchanged with external coastal waters (Edwards and Sharples 1985). Due to active mixing and tidal exchange, there is reduced likelihood of severe oxygen depletion in the water column.

An Atlantic salmon fish farm, located in the second basin (maximum depth: 49 m), has been active for 15 years. The site is farmed on a 2-year production: 2 years fallowed cycle, and the farm consisted of an array of 16 cages, each with a diameter of 25- and 15-m-deep nets. The maximum consented farmed biomass at the site was 1,500 tons of Atlantic salmon (Brigolin et al. 2008, 2009).

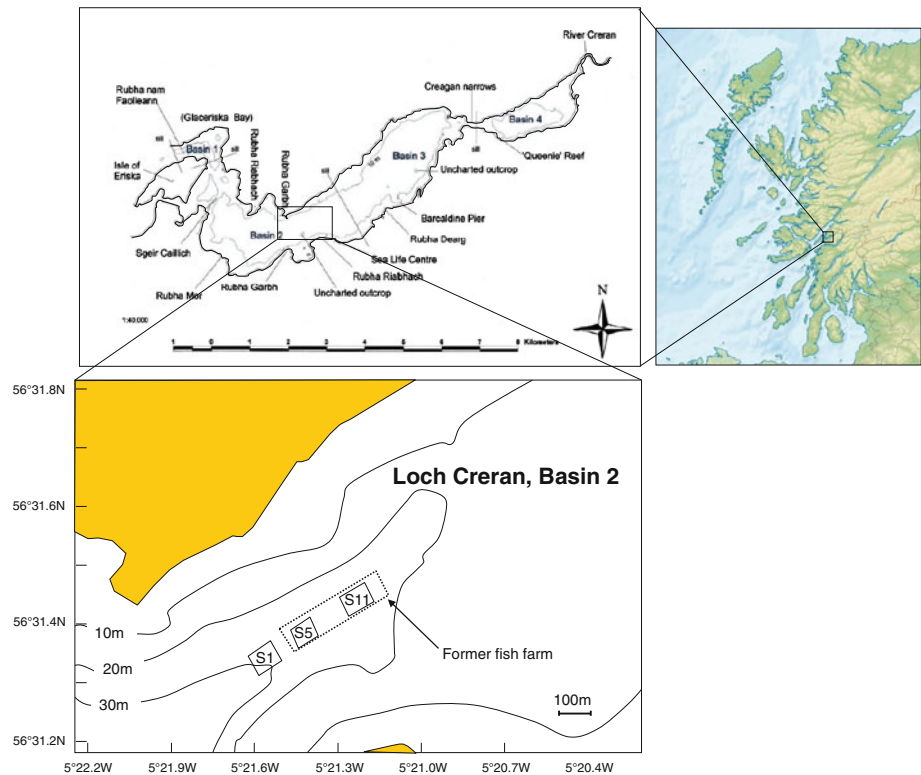


Fig. 1 Location of the sampling stations in Loch Creran

Table 1 Measurements performed during 2006 in Loch Creran

	Station S1	Station S5	Station S11
March	CHN analyses	CHN analyses	CHN analyses
May	5 O ₂ microprofiles	3 O ₂ microprofiles	1 O ₂ microprofiles
	3 resistivity profiles	5 resistivity profiles	4 resistivity profiles
	1 porosity profile	1 porosity profile	1 porosity profile
	4 benthic chamber incubations		6 benthic chamber incubations
	1 OC profile	1 OC profile	1 OC profile
	Abundance and biomass of bacteria		Abundance and biomass of bacteria
	1 planar optode deployment (48 h) (78 profiles extracted)		1 planar optode deployment (48 h) (80 profiles extracted)
August	5 O ₂ microprofiles	9 O ₂ microprofiles	5 O ₂ microprofiles
September	3 O ₂ microprofiles	7 O ₂ microprofiles	7 O ₂ microprofiles
		2 H ₂ S and 2 pH microprofiles	
October	CHN analyses	CHN analyses	CHN analyses
	Bacteria and viruses abundance		Bacteria and viruses abundance

2.2 Field Sampling Cruises

Most of field sampling and measurements were taken on board the RV *Calanus* and RV *Seòl Mara* during three cruises in May, August and September 2006. Additional cruises in March and October 2006 were used to collect sediment cores for bacteria and organic carbon content. Based on an initial survey in March using a Sediment Profile Imaging camera (SPI, Teal et al. 2008; Godbold and Solan 2009), sampling stations were selected to describe a gradient of organic matter enrichment linked to the fish farm activity, which had ceased its production in January 2006. The seabed around and in the footprint of the fish farm, the area directly beneath the cage group, was examined and three stations were selected (S1, S5 and S11). Station S1 was located outside the fish farm footprint and was considered as a reference station, reflecting background sedimentary conditions in the loch, whereas S5 and S11 were situated within the boundary of the vacated fish farm location (Fig. 1) and showed evidence of organic enrichment and a thinner sediment mixed layer (Godbold and Solan 2009). A complete list of the operations performed during the field expeditions is available in Table 1.

2.3 Sediment Coring, Organic Carbon Measurements and Porosity Determination

Undisturbed sediment cores were obtained using a Bowers and Connelly megacorer, which collected a maximum of 8 cores (Ø: 10 cm) per deployment (Barnett et al. 1984). Depth profiles of sediment organic carbon content were determined from a single core taken from each station (S1, S5 and S11) in March and again in October 2006. Sediment cores were sliced at 0.5-cm intervals between 0 and 2 cm, then 1-cm intervals down to 20 cm and stored frozen until freeze-dried in the laboratory. The decarbonation was performed using 10 % HCl and analysis was made with a LECO CHN 900 elemental analyser (Brigolin et al. 2009). Porosity was determined by subcoring one core with a 40-ml syringe which

was subsequently cut at 2 mm resolution for the first centimetre and 5 mm resolution down to 6 cm. Porosity was calculated from the weight of water loss after drying with a correction for dried salt and assuming a dry bulk density of 2.65 g cm^{-3} (Mienert and Schultheiss 1989), except for cores with elevated OC contents [i.e. S11 with OC > 4 % dry weight (d.w.)] where a value of 1.43 g cm^{-3} was adopted (Avnimelech et al. 2001; Bri-golin et al. 2009).

2.4 Bacterial Abundance and Biomass

Three undisturbed cores, from separate casts of the megacorer in each station, were sectioned onboard immediately after recovery and the upper 5 mm, 2–3 cm, 5–6 cm and 10–11-cm depth intervals were collected in sterile plastic bags. The samples were fixed with $0.02 \mu\text{m}$ filtered glutaraldehyde to a final concentration of 3 %. The samples were stored at in situ temperature and in the dark for a maximum of 2 h before processing. Bacterial cells were extracted from 25 g of sediment according to Middelboe et al. (2003), using sodium pyrophosphate (10 mM) and staining with SYBR Gold (Molecular Probes). Ten fields of view were counted from each sample under oil immersion at $1,000\times$ magnification using a Zeiss Axioskop equipped for epifluorescence.

2.5 In Situ Microprofiles

An autonomous benthic microprofiler (Unisense[®]) was used to perform in situ measurements of 1-D distribution of O_2 , resistivity, pH and H_2S at the sediment–water interface (SWI). The profiler was equipped with 4–5 O_2 microelectrodes and a resistivity probe (Unisense[®]). In September 2006, 1 H_2S microelectrode and 2 pH microelectrodes were added. The microprofiler deployments included 30-min resting time before measurement to allow any sediment disturbance to settle. Profiles of O_2 , resistivity, pH and H_2S were recorded at 50, 100 or 200 μm resolutions.

Dissolved oxygen concentration was measured by amperometric oxygen microelectrodes provided with a built-in reference and an internal guard cathode (Revsbech 1989). A detailed description of the O_2 microelectrode configuration, performance and calibration procedure is given in Lansard et al. (2009) and Cathalot et al. (2010). Briefly, the O_2 microsensors had outer tip diameters of 100 μm , stirring sensitivity of <1 %, 90 % response time of 10 s and less than 1 % per hour current drift. A 2-points linear calibration of the O_2 microelectrode signal was performed against O_2 concentration, measured by Winkler titration (Grasshoff et al. 1983), in the bottom water and in the anoxic zone of the sediment.

Resistivity measurements were taken with an electrode similar to that described by Andrews and Bennett (1981) and Dedieu et al. (2007). A prior calibration of the voltage outputs was made by measuring the probe's signal in KCl standard solutions. Resistivity recordings were then converted to the inverse formation factor (F^{-1}) values using the equation of Berner (1980):

$$F^{-1} = \frac{R_{bw}}{R_z}$$

where R_{bw} is the average resistivity in bottom water and R_z is the mean resistivity at a given depth z . The inverse formation factor was translated into porosity (ϕ) using the empirical Archie's law: $F^{-1} = \phi^m$ (Ullman and Aller 1982), where m is determined experimentally by the type of sediment.

Concentrations of dissolved sulphide (H_2S) in the sediment were measured using H_2S microelectrodes (Unisense[®]). Sulphide microelectrodes are Clark-type microsensors with a platinum guard cathode to ensure a low and stable zero-current: they had outer tip diameters of 100 μm , stirring sensitivity of <2 %, 90 % response time of 10 s and less than 2 % per hour current drift. Microelectrode calibration was accomplished using H_2S standards prepared daily from a main solution and preserved with TiCl_3 . The main sulphide solution was re-titrated by the classical sulphide titration every day (Grasshoff et al. 1983). The position of the SWI for sulphide electrode was determined using the resistivity probe and the relative positions of the H_2S and resistivity electrodes. This latter had been determined when mounting the electrodes on the profiler. Because of the bottom topography exhibited in the planar optode images, the error in H_2S position was assumed to be $\pm 2\text{--}3$ mm.

pH measurements were taken using microelectrodes manufactured by Unisense[®] with a tip diameter of 100 μm and a reference electrode made of a simple open-ended Ag/AgCl electrode. Calibration was performed daily using three NBS pH standard buffer solutions (pH 4, 7 and 9) covering the range of measurements. All calibration responses were linear from pH 4 to pH 9 with a slope between 55 and 59 mV/pH units. As pH standard solutions in artificial sea water were not used in this study, we report measurements as ΔpH , which is the variation of pH with regard to bottom water. To assess the drift of the electrode, measurements were taken in bottom water both before and after the profile and we checked that the electrode signal variation was less than 10 %.

2.6 Planar Optode

We used an autonomous custom-made planar optode mounted on a tripod frame to record 2-D time-series images of oxygen distributions in situ within the sediment. The planar optode module was the same as the one described by Glud et al. (2001). Briefly, O_2 quenchable photophores made of ruthenium complexes ($\text{Ru}(\text{diph})_3$, ruthenium (III)-Tris-4,7-diphenyl-1,10-phenanthroline) emitting red radiations when excited in blue wavelengths were coated with PVC and trapped in a transparent polyester support. The planar optode was therefore a double layer and consisted of the support plate and the photophore layer. Intensity and signal lifetime are inversely proportional with the surrounding oxygen concentration (Glud et al. 2001, 2005). During each deployment, a set of calibration pictures were taken in the bottom water before moving down into the sediment. In this study, we focused on luminescence lifetime images to quantify the 2-D oxygen distribution. Images were calibrated from bottom water oxygen concentration and sediment images (used as references values) using the Stern–Volmer equation:

$$\frac{\tau_0}{\tau} = 1 + K_q \cdot [\text{O}_2]$$

With τ_0 being the quenching duration in the absence of oxygen, K_q the extinction coefficient (with $K_q = k_q \cdot \tau_0$ where k_q is the real extinction constant).

Images taken in the water column and the deep anoxic zone of the sediment gave us values of τ at 100 and 0 % of oxygen saturation, respectively. During each deployment, a set of 4 successive O_2 images were taken every 4 h. Only the last image was used to determine oxygen distribution in order to ensure steady-state conditions (Glud et al. 2001). It was possible to extract 640 vertical profiles on a single image, each profile corresponding to one line of pixels. In order to decrease the profiles' noise and improve their quality, a 2-D Savitzky-Golay smoothing filter was applied: each extracted profile corresponded to

the average of 5 adjacent profiles and thus covers a 1.1-mm distance on the oxygen images. Random O₂ profiles were extracted from each image. The number of O₂ profiles extracted depended on the image's quality and signal noise. A total of 158 profiles were therefore extracted (excluding damaged sections and active irrigation).

2.7 Diffusive Flux Calculations

Oxygen profiles, from both microelectrodes and planar optode images, were used to calculate the diffusive oxygen uptake (DOU) rate of the sediment, which was assessed using two different methods. The first was to calculate the diffusive oxygen fluxes at the sediment–water interface (SWI) using Fick's first law:

$$\text{DOU} = F^{-1} D_0 \left[\frac{d\text{O}_2}{dz} \right]_{z=0}$$

where D_0 is the molecular diffusion coefficient in sea water at in situ temperature, $\left[\frac{d\text{O}_2}{dz} \right]_{z=0}$ is the oxygen gradient at the SWI determined by linear regression over 50- or 100- μm intervals (depending on the profile resolution) and F^{-1} is the inverse formation factor at the SWI.

The second way to calculate the DOU is by using the PROFILE software (Berg et al. 1998): its curve fitting approach allows estimation of the consumption rates with depth by adjusting the calculated oxygen profile to the observed one. A normalisation to a temperature of 9 °C was made using the relationship proposed by Hetland and Dimarco (2008) and modified to account for a Q_{10} of 2.5 (Dedieu et al. 2007) using:

$$\text{DOU}_T = \frac{\text{DOU}_{T_i}}{2.5^{\left(\frac{T_i - T}{10}\right)}}$$

where $Q_{10} = 2.5$, DOU_{T_i} is the diffusive demand of oxygen at initial temperature T_i , T_i is the initial temperature and T is the final temperature. With the T values observed here (9 °C in May and 14 °C in summer), the normalisation factor amounts to 1.6 (Table 3).

2.8 Incubations with In Situ Benthic Chambers

In situ benthic chambers were used to determine total oxygen uptake (TOU) rate, together with the benthic DIC flux. A titanium benthic frame designed for full ocean depth (Ståhl 2001; Apler 2007; Tengberg et al. 2004) was equipped with four-square incubation chamber modules (400 cm²). We collected 10 syringes of water samples which were analysed for DIC within a few hours after recovery. Oxygen optodes (Aanderaa[®]) measured the oxygen concentration in the water of the chambers during the incubations at 1-min intervals. They were cross-calibrated with Winkler titrations. Mixing of the water in the chamber was carried out by a paddle wheel placed centrally in the chamber. During incubations, the stirring was slow, creating a low shear velocity of approximately 0.5 cm s⁻¹. Five deployments ranging from 24 to 48 h were made during the May 2006 campaign. At each deployment, several repeated incubations were done: the lids of the chambers were opened between each incubation to flush the overlying water in the chambers.

The chamber water volume was measured: (1) by collecting the incubated sediment and water and measuring the height of the overlying water, and (2) by injecting 60 ml of

Table 2 Environmental parameters measured in Loch Creran in May, August and September 2006

Parameter	May 2006		August 2006	September 2006
	Surface water	Bottom water	Bottom water	Bottom water
T (°C)	/	9.2	14.0	14.1
Salinity (PSU)	/	32.7	33.2	32.2
O_2 ($\mu\text{mol l}^{-1}$)	318 ± 12	297 ± 15	245 ± 15	243 ± 1
Chl <i>a</i> ($\mu\text{g l}^{-1}$)	133 ± 45	61 ± 27	/	/

bromide (300 mM) solution into each chamber at the start of the incubation and measuring its dilution after 30 min. The syringe water samples were filtered through pre-rinsed 0.45- μm pore size cellulose acetate filters and then titrated for oxygen with a precision of 0.5 % and for DIC using an automated system based on non-dispersive infrared detection of CO_2 after acidification of sample in a 4-ml sampling loop. A certified reference material (CRM, provided by A. Dickson, Scripps Institution of Oceanography, USA) was used for calibration and correction for system drift every fifteen samples. The analytical precision was 0.2 % RSD ($n = 15$) or better.

The TOU was calculated assuming a linear concentration change in the chamber over time. The slope of the best fit line was achieved by a least square linear regression of 30 oxygen measurements which were taken 10 min after the start of the incubation at 1-min intervals. The slope was then multiplied by the overlying water height in the chamber. The same procedure was used for DIC fluxes, except that measurements of all syringe DIC samples were used in the calculation of the slope. The uncertainty of each flux was calculated by using the standard error of the slope, large uncertainties reflecting scatter of the individual data points.

3 Results

3.1 Environmental Parameters

Salinity was around 33 PSU during all cruises (Table 2). Table 2 shows that bottom water temperatures warmed up from 9.2 to 14.1 °C between May 2006 and August/September 2006. May corresponds to the beginning of spring and the seasonal warming just began at the end of our expedition. Such an increase in bottom water temperature induces a reduction of oxygen solubility by 50 $\mu\text{mol l}^{-1}$ from spring to summer. In May, chlorophyll *a* (Chl*a*) concentrations were relatively high in surface ($>100 \mu\text{g l}^{-1}$) and bottom ($<100 \mu\text{g l}^{-1}$) water.

3.2 Porosity and Formation Factors

Porosity profiles (Fig. 2) exhibited a classical decrease from the SWI to the deep sediment. Porosity values differed for stations S1 and S5, with an asymptotic porosity at 5-cm depth below 0.7 for station S1 and around 0.75 for station S5. S11 showed a two-step decrease with a rapid decrease in the first centimetres from 0.95 to 0.85 and a second decrease below 3 cm to reach values below 0.6. Comparisons were made with porosity calculated by the resistivity profile. Ullman and Aller (1982) estimated that the m coefficient was about 2.5–3 in coastal muddy sediment with porosity around 0.7. We adjusted the m value for

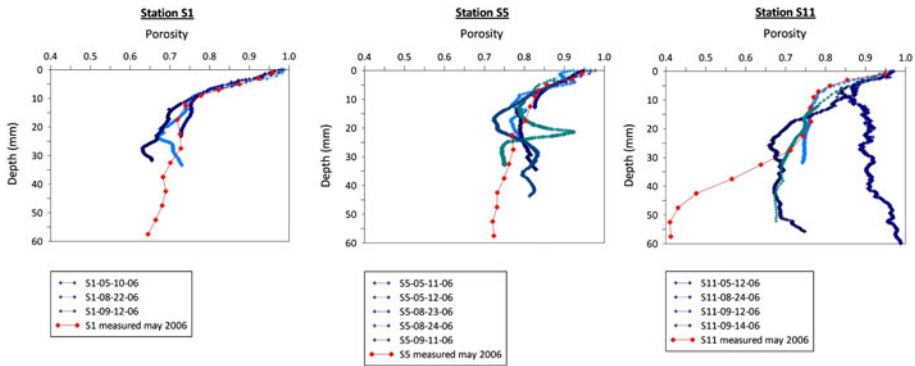


Fig. 2 Porosity profiles acquired during all cruises: *solid line with plus* profiles derived from resistivity measurements, formation factor and Archie's law. *Solid line with minus* profiles were measured directly on samples from sediment cores

each station in order to match the observed porosity profiles. In all cases, m was approximately 3. Adjustments were satisfactory except for station S11.

3.3 Sediment Organic Carbon (OC) Content and C/N Ratio

A large difference in OC content was observed between stations (Fig. 3). For both seasons over the first 2 centimetres, station S1 showed the lowest OC content with 1.5 ± 0.1 % d.w., station S5 showed an intermediate OC content with 2.7 ± 0.4 % d.w. and station S11 showed the highest OC content with 6.6 ± 1.1 % d.w. Stations S11 and S5 had high OC contents at the top of the sedimentary column and lower values at 10-cm depth. The low values recorded at deeper intervals may reflect the background composition of the sediments: 1.6 % at S5 and 1.4 % at S11 in the 10–20-cm depth interval. These values are similar to the average OC content recorded at S1 (1.5 %). On a seasonal basis, March and October were similar with a gradient of OC concentration from S1 to S11.

C/N molar ratio varies between 8 and 10 with an average value of 8.6 ± 1.1 in the upper 2 cm of the sediment at all stations in March 2006 and slightly lower values at station S11 (7.6). C/N ratios were larger in October 2006 as they reached values of 9–10 at Station S1 and S5, but were still around 8 at S11.

3.4 Bacterial Data

Figure 4 shows the seasonal abundance of bacteria at the two main sampling stations (S1 and S11) in May and October 2006. Each data point represents the mean of three replicate cores to account for spatial heterogeneity. There was a general increase in bacterial number between May and October 2006 in the Loch Creran sediments linked to the temperature increase (Pomeroy and Wiebe 2001). In most instances, station S11 exhibited slightly higher bacterial abundance than S1. S11 had the highest abundance of bacteria at mid-depths in May and presented a maximum abundance of 4×10^8 bacteria g^{-1} wet sediment at mid-depth in October.

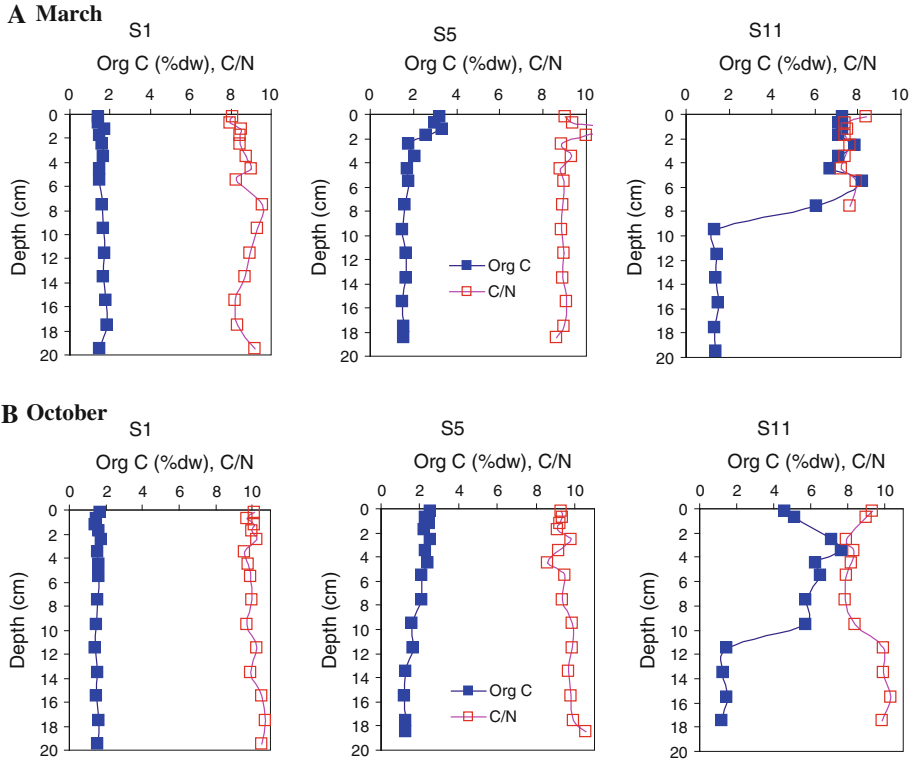


Fig. 3 Distribution of organic carbon (OC, % d.w. closed squares) and C/N molar ratio (open squares) in sediment cores of the Loch Creran (**a** March and **b** October)

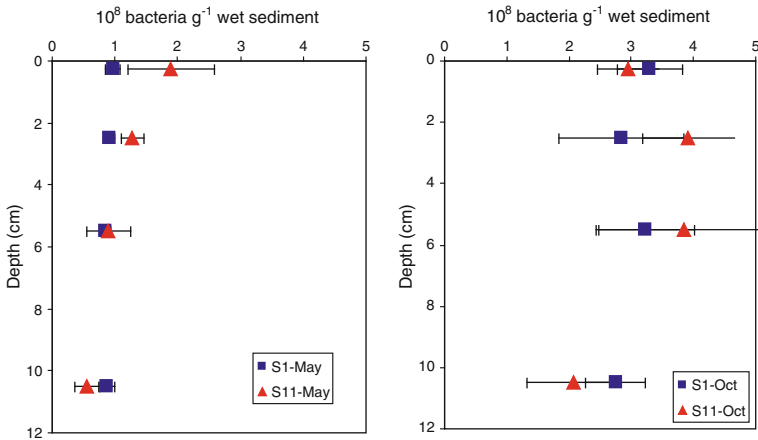


Fig. 4 Bacterial abundance in Loch Creran sediments at stations S1 (squares) and S11 (triangles). *Left* May 2006. *Right* October 2006

3.5 Microprofiler: Diffusive Oxygen Uptake (DOU) and Sulphide Profiles

A total of 44 oxygen profiles were acquired during the 3 field expeditions. They all showed a decrease in O_2 concentration with depth indicating net oxygen consumption in the sediment (Fig. 5). Variations at the station scale are clearly illustrated by the variable oxic gradients and oxygen penetration depths (OPDs). Among all profiles, OPD ranged from 0.3 to 3 mm with shallower OPD observed at station S5 and S11 (average of 1.2 ± 1.5 and 0.9 ± 0.4 mm, respectively) and larger OPD at station S1 (average of 2.1 ± 0.4 mm). The shallowest OPDs were measured during August and September 2006, that is, during the warmer period, but due to the small number of profiles collected in May ($n = 8$), it is not clear if this pattern is prevalent across the stations. A two-tailed t test showed that OPDs at stations S5 and S11 were not significantly different ($p > 0.05$). In contrast, there was a significant difference when S5 and S11 were pooled and compared to station S1 ($p < 0.05$): the sediment collected from the vacated fish farm site had thinner oxic zones than those located on the 'reference' station S1.

Average DOU values at station S1 were $21 \pm 5 \text{ m}^{-2} \text{ day}^{-1}$ ($n = 7$, Table 3; Fig. 6) for the late summer period. Average DOU at the impacted stations S5 ($78 \pm 25 \text{ mmol O}_2 \text{ m}^{-2} \text{ day}^{-1}$, $n = 16$) and S11 ($63 \pm 37 \text{ mmol O}_2 \text{ m}^{-2} \text{ day}^{-1}$, $n = 12$) for the summer period was approximately three to four times higher than the reference station (S1) at the same period. There is no significant difference for the DOU values ($p > 0.05$) between S5 and S11. As for OPDs, DOU values at station S1 were statistically different from values in stations S5 and S11 when pooled together ($p < 0.05$). Data from station S5 and S11 appeared to display a bimodal distribution. Different profiler deployments within the same station gave either large fluxes ($>60 \text{ mmol O}_2 \text{ m}^{-2} \text{ day}^{-1}$) or intermediate fluxes (around $40 \text{ mmol O}_2 \text{ m}^{-2} \text{ day}^{-1}$). This is evidenced on Fig. 6 with hatched bars showing the intermediate values obtained on a single deployment. These features were consistent with the DOU values calculated with PROFILE (data not shown). Differences between the two methods were less than 10 %, confirming the validity of the SWI positioning.

Four sulphide profiles were acquired in September 2006. H_2S was only present on the 2 profiles performed at S11 (in the range of depths studied, i.e., 5 cm): the other 2 profiles indicated that porewater of the upper sediments at S5 and S1 did not contain dissolved sulphide. The two profiles at S11 (September 12 and 14) showed an increase in the H_2S concentration from 0 μM up to 400–1,000 μM at 33- and 18-mm depth, respectively (Fig. 7). In Fig. 7a, H_2S was detected at 3-mm depth and the mean DOU for this deployment was $117 \pm 7 \text{ mmol O}_2 \text{ m}^{-2} \text{ day}^{-1}$, the highest DOU recorded in this study. The pH profile (Fig. 7c) measured alongside displayed a large decrease by more than 1.3 pH units with a sharp decrease occurring over 1 mm below the SWI, followed by an increase in pH and a slower decrease down to 2 cm. As some drift was recorded for this electrode (around 0.3 pH unit), the trend in the bottom water and below 2 cm is attributed to this drift. The other H_2S profile obtained in S11 displayed a deeper depth of H_2S appearance (18 mm) with lower concentrations ($<500 \mu\text{M}$): it was associated with an OPD of 1.0 mm and an average DOU of $50 \pm 20 \text{ mmol O}_2 \text{ m}^{-2} \text{ day}^{-1}$.

3.6 Planar Optode

Planar optode data measured in situ showed irregular microtopography of the SWI and variable OPDs directly viewable on oxygen images (Fig. 8). The DOU rates calculated from planar optode images collected in May were $11.1 \pm 2.6 \text{ mmol O}_2 \text{ m}^{-2} \text{ day}^{-1}$ ($n = 78$) at station S1 and $14.6 \pm 2.5 \text{ mmol O}_2 \text{ m}^{-2} \text{ day}^{-1}$ ($n = 80$) at station S11.

Fig. 5 All oxygen profiles measured during May, August and September 2006 in Loch Creran at the three station S1 (reference), S5 and S11 (fish farm). Differences in bottom water reflect the seasonal variations in temperature and oxygen concentrations in the environment

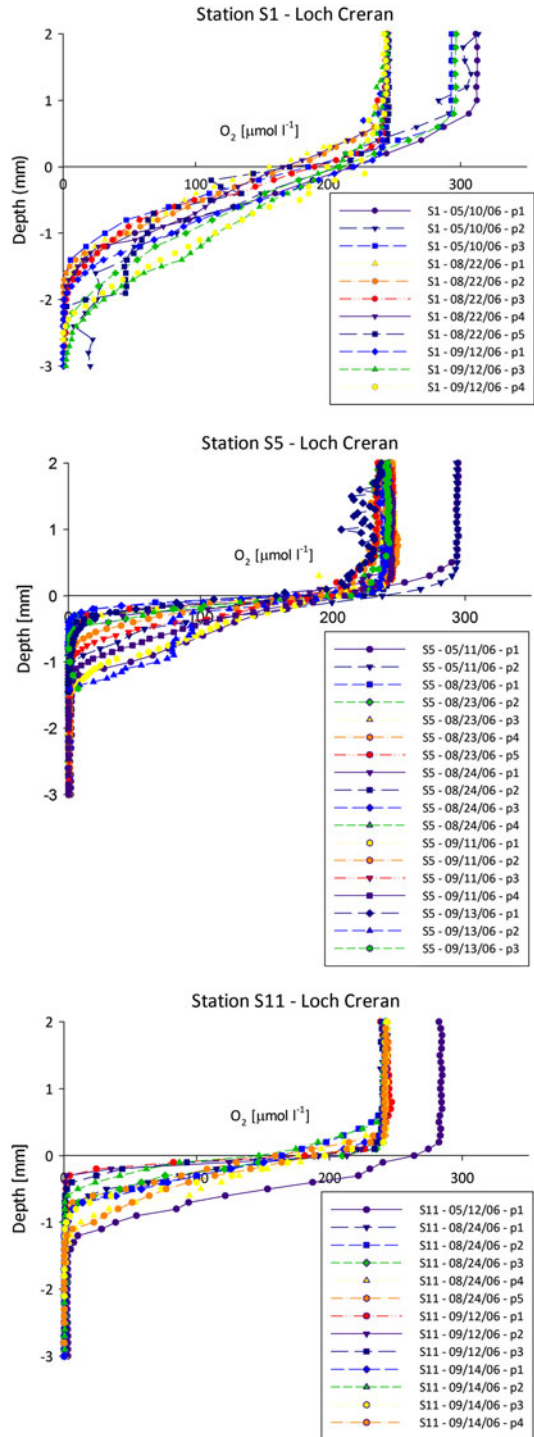


Table 3 In situ benthic oxygen fluxes for all stations at different seasons: total oxygen uptake (TOU) measured by benthic chambers and diffusive oxygen uptake (DOU) derived from O₂ electrodes microprofiles

Total oxygen uptake (mmol O ₂ m ⁻² day ⁻¹)						
Spring 2006						
May						
S1	2-May	23.6	4-May	32.6		
	2-May	23.8	4-May	29.2		
	2-May	21.9	4-May	34.0		
	2-May	25.0	4-May	36.5		
	avg	23.6 ± 1.3	avg	33.1 ± 3.0		
S11	7-May	29.6	9-May	62.1	11-May	67.9
	7-May	26.0	9-May	46.6	11-May	51.9
	7-May	23.2	9-May	49.2	11-May	42.0
	7-May	23.4	9-May	50.2	11-May	62.2
	avg	25.6 ± 3.0	avg	52.0 ± 6.9	avg	56.0 ± 11.4

Table 3 continued

		Diffusive oxygen uptake ($\text{mmol O}_2 \text{ m}^{-2} \text{ day}^{-1}$)				
		Late summer 2006				
Spring 2006		August		September		
May		August		September		
S1	10-May	15.7	22-Aug	20.5	12-Sept	18.3
	10-May	16.1	22-Aug	18.1	12-Sept	18.5
	10-May	20.3	22-Aug	20.6	12-Sept	32.7
	10-May	15.4	22-Aug	18.5		
	avg	16.9 ± 2.3	avg	19.4 ± 1.3	avg	23.1 ± 8.3
S5			avg 9 °C	12.3 ± 0.84	avg 9 °C	14.6 ± 5.22
	11-May	27.9	23-Aug	88.1	11-Sept	38.0
	11-May	39.3	23-Aug	80.7	11-Sept	53.1
			23-Aug	101.9	11-Sept	44.8
			23-Aug	81.6	11-Sept	53.3
S11			23-Aug	80.2	24-Aug	45.6
	avg	33.6 ± 8.1	avg	86.5 ± 9.2	avg	47.3 ± 7.3
			avg 9 °C	54.7 ± 5.79	avg 9 °C	29.9 ± 4.64
	12-May	24.8	24-Aug	52.1	12-Sept	121.4
			24-Aug	27.4	12-Sept	109.1
		24-Aug	77.7	12-Sept	119.0	
		24-Aug	21.5	14-Sept	46.9	
		24-Aug	35.8	14-Sept	73.6	
avg	$24.8 \pm -$	avg	42.9 ± 22.6	avg	116.5 ± 6.5	
		avg 9 °C	27.1 ± 14.3	avg 9 °C	73.7 ± 4.11	
				14-Sept	34.5	
				14-Sept	30.4	
				14-Sept	46.4 ± 19.5	
				14-Sept	29.3 ± 12.3	

Results are reported at in situ temperature (9 °C in May and 14 °C in August–September). Italics indicate low impact and bold indicates high impact from the fish farm (see Sect. 4 for details). For the late summer values, a normalisation was performed using a normalisation factor for temperature calculated as $2.5^{(14-9)/10}$ which equals 1.6. In the Table, 'avg 9 °C' indicates the average DOU value within a single deployment normalised for a 9 °C temperature

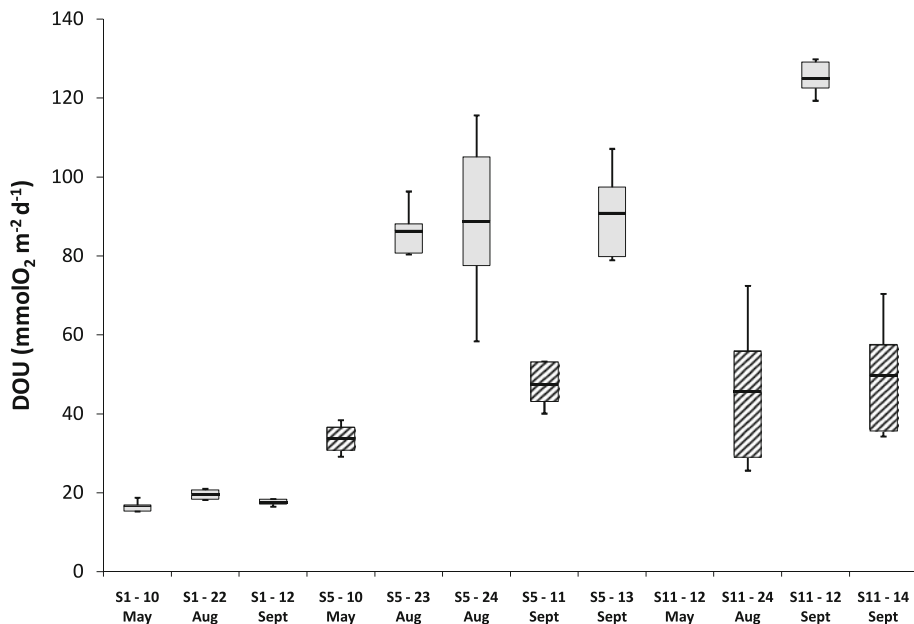


Fig. 6 Diffusive oxygen fluxes distribution for the 3 periods of observation pooled by station plotted in *Whisker plots*. For S5 and S11, *hatched bars* indicate lower than average fluxes to highlight the bimodality existing at the impacted site. *Each date* indicates one profiler deployment. *Bottom and top of the boxes* are the 25th and 75th percentiles. The *middle bars* in the *boxes* are the average values and the *error bars* extend to the 10th percentile for the lowest and 90th percentile for the top

As previously observed for the microelectrode DOU fluxes, these diffusive fluxes were higher beneath the vacated fish farm site. A two-tailed *t* test showed that fluxes at S1 and S11 were statistically different ($p < 0.05$). This tendency was also indicated by the OPDs, which were shallower on S11 (average of 2.16 ± 0.83 mm) than on S1 (average of 3.48 ± 0.61 mm).

The variability of DOU rates was observed at both stations S1 and S11, in a single set of measurements (i.e. one image), using the coefficient of variation (CV = standard deviation/average) which gives an estimation of the dispersion of the variable; for instance, the CV was about 18 % at station S11 (Fig. 8a). In comparison, the CV factor was 14 % at station S1 (Fig. 8b).

3.7 Benthic Chambers Measurements

TOU rates were calculated from benthic chamber measurements taken at stations S1 and S11 in May 2006 (Table 3). The results show larger TOU at the impacted station than at the reference site (S1: TOU = 30 ± 6 mmol O₂ m⁻² day⁻¹, S11: TOU = 46 ± 12 mmol O₂ m⁻² day⁻¹). A nonparametric Mann–Whitney test showed that TOUs at the two stations are statistically different ($p < 0.01$).

A bimodal distribution was found at station S11: TOU measurements of May 9 and 11 were substantially larger than TOU on May 7. Comparison between TOU measured in May 2006 and microprofiles DOU measured in August/September 2006 is discussed later as the temperature difference was noticeable (9 °C in May vs. 14 °C in August/September).

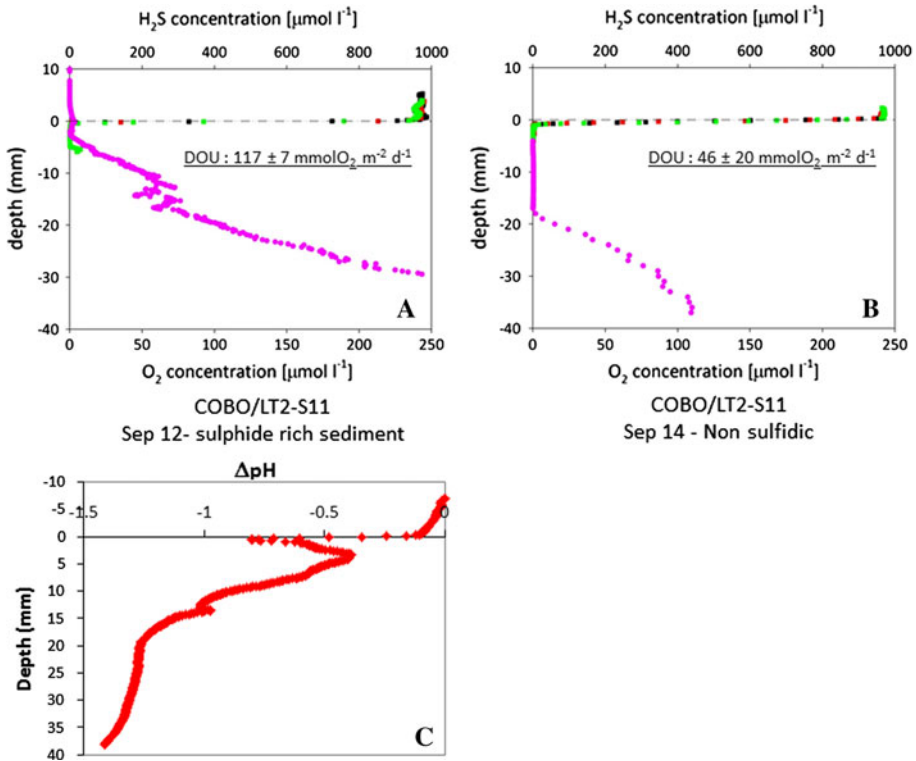


Fig. 7 a, b H₂S, O₂ profiles performed at station S11, 12 and 14 September 2006, respectively. c pH profile measured in sediments from S11 on September 12

As for TOU, measurements of benthic DIC fluxes were taken in May 2006 at stations S1 and S11 (Table 4). There were two valid incubations at station S1, which showed average DIC fluxes of $20 \pm 5 \text{ mmol C m}^{-2} \text{ day}^{-1}$ ($n = 2$). DIC fluxes were $41 \pm 27 \text{ mmol C m}^{-2} \text{ day}^{-1}$ ($n = 10$) at S11. Unlike TOU and DOU, DIC fluxes displayed no clear trend for the deployments, mainly due to the high variance of fluxes in each deployment. The ratio between the average DIC and oxygen fluxes at each station displayed large variations (Table 4). The DIC/O₂ ratio was on average 0.85 ± 0.3 for both station.

4 Discussion

4.1 Comparisons Between In Situ Profiling Techniques

Two in situ profiling techniques, based on single microelectrodes profiling and planar optode imaging, were used during this study. The methodological issues arising from each technique have been discussed in previous studies (Lansard et al. 2003; Tengberg et al. 1995; Glud et al. 2005; Boudreau and Jørgensen 2001; Rabouille et al. 2003) and thus will only be briefly covered here.

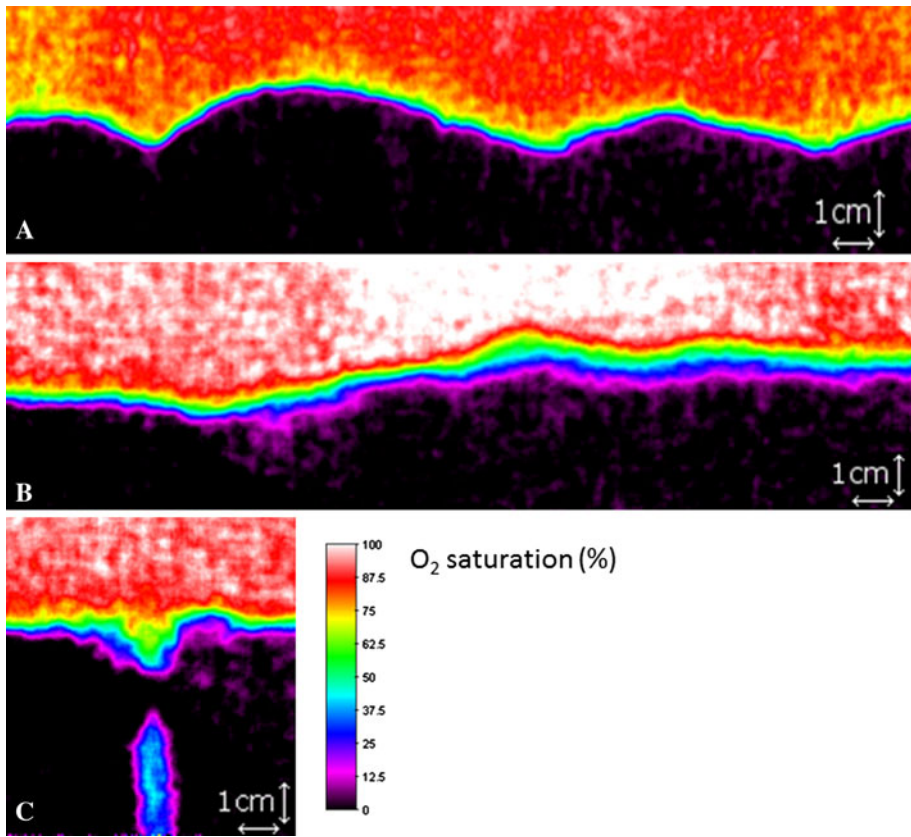


Fig. 8 Planar optode oxygen images; **a** heterogeneous microtopography at S11; **b** irregular penetration depth at S1; **c** burrow at S1

Table 4 Summary of oxygen and DIC fluxes measured with in situ benthic chambers at station S1 and S11 in May 2006, and the associated DIC/O₂ flux ratios

Station	O ₂ flux (mmol O ₂ m ⁻² day ⁻¹)	DIC flux (mmol C m ⁻² day ⁻¹)	DIC/O ₂ ratio
S1	21.9 ± 0.9	23.2 ± 6.7	1.1
S1	25.0 ± 0.9	16.6 ± 5.4	0.7
S11	29.6 ± 5.6	36.2 ± 5.4	1.2
S11	26.0 ± 4.2	10.2 ± 3.7	0.4
S11	23.4 ± 4.1	17.5 ± 14.1	0.7
S11	62.1 ± 2.1	101 ± 75.4	1.6
S11	46.6 ± 1.2	25.5 ± 10.9	0.5
S11	49.2 ± 1.1	52.3 ± 41.3	1.1
S11	67.9 ± 2.8	63.6 ± 10.4	0.9
S11	51.9 ± 1.7	23.8 ± 1.8	0.5
S11	40.2 ± 2.0	26.3 ± 14.6	0.7
S11	62.2 ± 2.0	49.4 ± 1.7	0.8

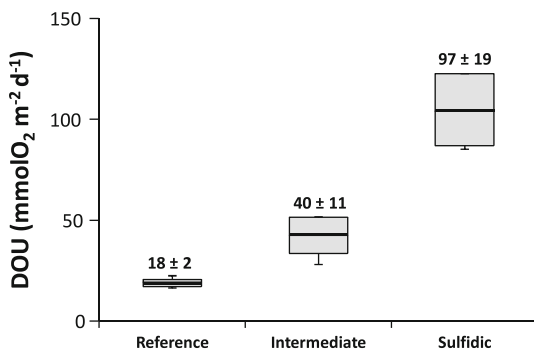
For microelectrode measurements, the variations in DOU values observed within a single deployment most likely results from natural spatial heterogeneity: in such high porosity environment, the uncertainty associated with the SWI positioning is unlikely to significantly affect the calculated fluxes (Reimers and Smith 1986). Similarly, planar optode images highlight an important microspatial heterogeneity in the sediment. A single set of profiles displayed a wide range of OPDs and diffusive oxygen fluxes. Hot spots of organic matter degradation, from millimetre to centimetre scale, are tightly linked to oxygen consumption (Rabouille et al. 2003; Glud et al. 2009) both by carbon mineralization and oxidation of reduced compounds. The large variability in DOU rates on single deployment likely arises from the microheterogeneity in the sediment.

Oxygen microprofiles extracted from planar optode images displayed a thicker diffusive boundary layer (DBL) and a noisier top part. Indeed, compaction as the optode enters the sediment, edge effects, changes in the local currents and alteration of the sediment surface structure affect the oxygen distribution in the DBL (Glud et al. 2001). Nevertheless, we found a $\frac{\text{SWI O}_2 \text{ concentration}}{\text{bottom water O}_2 \text{ concentration}}$ ratio of 0.75 ± 0.11 indicating that the DBL thickness did not significantly influence the DOU fluxes during the planar optode deployments (Boudreau and Jørgensen 2001; Røy et al. 2002; Wenzhofer and Glud 2004; Tengberg et al. 2004).

4.2 Spatial Heterogeneity in the Area Impacted by the Fish Farm

As expected, the sediment impacted by the fish farm (stations S5 and S11) showed larger oxygen uptakes than the reference station and a large spread of DOU rates (Fig. 6). The DOU values range from 25 to 123 $\text{mmol O}_2 \text{ m}^{-2} \text{ day}^{-1}$ (Fig. 6; Table 3), and deployments were statistically different (Kruskall–Wallis test, $p < 0.01$, $n = 31$) highlighting a spatial heterogeneity within the station at the metre scale (i.e. between deployments within S5 and S11). Nevertheless, S5 and S11 were not statistically different (Mann–Whitney on DOU rates, $p > 0.05$, $n = 31$). We therefore pooled the DOU rates from both stations and split them into two groups of deployments shown by plain and hatched bars (Fig. 6): one group with intermediate oxygen fluxes ($< 60 \text{ mmol O}_2 \text{ m}^{-2} \text{ day}^{-1}$) and the other one with high fluxes ($> 80 \text{ mmol O}_2 \text{ m}^{-2} \text{ day}^{-1}$). This arrangement is statistically relevant (Kruskall–Wallis, $p < 0.01$, $n = 31$) and DOU rates can thus be grouped from intermediate fluxes (average $40 \pm 11 \text{ mmol O}_2 \text{ m}^{-2} \text{ day}^{-1}$) to large fluxes ($97 \pm 19 \text{ mmol O}_2 \text{ m}^{-2} \text{ day}^{-1}$) for the summer period (Fig. 9). The spatial heterogeneity observed at these stations can be related to the patchy deposition pattern of unused fish food and fish faeces (Hargrave et al. 1997; Lu and Wu 1998). In fact, unused fish food and faeces have higher deposition rates

Fig. 9 Resorted sites with average and standard deviations of oxygen fluxes in Loch Creran sediments



below the fish cages and lower accumulation rates in between cages (Brigolin et al. 2009). This patchiness at the station scale (metre) allows us to consider station S5 and S11 as a single but heterogeneous impacted site (referred as S5/S11) with intermediate and large disturbance.

Despite the small number of observations, the dual nature of the impacted sediment site is also evidenced by the TOU rates measured by benthic chambers. Deployments in May at station S11 consistently showed two groups of fluxes (Table 3) with May 7 deployment being in the intermediate range and May 9 and 11 deployments being in the higher range. In order to compare these fluxes to the DOU rates measured by microelectrodes in August and September, a normalisation to a temperature of 9 °C was made using the relationship proposed by Hetland and Dimarco (2008) and Dedieu et al. (2007) (Table 3).

As mentioned above, TOU rates in May are split between a group of intermediate fluxes around 40 mmol O₂ m⁻² day⁻¹ at 14 °C and a group of high fluxes around 80–90 mmol O₂ m⁻² day⁻¹ at 14 °C. These fluxes are in the same range as the DOU rates observed in August–September and display the same bimodal distribution with intermediate and large fluxes.

The TOU/DOU ratio at the reference station (S1) was 1.7, highlighting the importance of irrigation and bioturbation by benthic macro and meiofauna in the reference station. The impacted station S5/S11 displayed a TOU/DOU ratio around 0.9, discarding irrigation as a major process in this sediment. This value close to 1 holds for both the intermediate and the highly impacted sites of S5/S11. It reflects the exclusion of large macrofauna and hence the predominance of intense microbial mineralization activity of both oxic and anoxic bacterial processes (e.g. sulphate reduction) and the reoxidation of dissolved reduced components. The differences in TOU/DOU ratios highlight again the station scale variability with two distinct types of benthic habitats without and within the footprint of the vacated fish farm: well-oxygenated macrofauna dominated versus macrofauna-excluded/microbially driven sediment, respectively. Under the vacated fish farm, highly sulphidic sediments with DOU rates up to 125 mmol O₂ m⁻² day⁻¹ were found. Visual inspection of the muddy sediment in this area revealed largely sulphidic with fine-grained black smelly sediments. Scuba divers also reported the presence of *Beggiatoa* spp. bacterial mats on the sea floor, which are well known to live in sulphur-rich environments of the Loch Creran (Nickell et al. 2003).

Spatial heterogeneity was also evident within the impacted S5/S11 station as some sediment associated with lower oxygen fluxes (September 11.) showed the absence of dissolved sulphide over the first 5 cm. Similarly, Fig. 7b reveals an increase in H₂S concentration 18 mm below the SWI, indicating a moderate sulphate reduction–based mineralization, commonly found in naturally OC-rich coastal systems. In highly impacted areas, sediment cores were black with a strong H₂S smell and displayed little visual evidence of living macroinfauna. In March 2006, a SPI deployment at station S11 showed a loose and flocculent black anoxic sediment which appeared to be anoxic (Godbold and Solan 2009), corresponding to what is referred to as ‘fish farm sediment’ by many authors (Mulsow et al. 2006; Brooks et al. 2004; Brooks and Mahnken 2003). H₂S microprofiles performed in September at station S5/S11 showed an increase in sulphide concentration from only a few mm below the SWI (Fig. 7a). High H₂S levels up to 1 mM at 3-cm depth are indicative of strong organic carbon mineralization by sulphate-reducing bacteria in the anoxic sediment (Mulsow et al. 2006; Brooks et al. 2004; Brooks and Mahnken 2003).

Similarly, the DIC/O₂ ratio obtained during benthic chambers deployments (Table 4) did not show any clear pattern. Close to 1 at S1, it indicates the predominance of aerobic mineralization processes at the reference site. Oscillating between 0.4 and 1.6 at the

Table 5 Comparison of sediment oxygen uptake rates under different fish farm sites

Study	Site	Oxygen fluxes
(Pamatmat and Bhagwat 1973)	Clam Bay (SW Canada)	DOU: 166–179 mmol O ₂ m ⁻² day ⁻¹
Hall et al. 1990	Gullmar Fjord (W Sweden)	TOU: 90–180 mmol O ₂ m ⁻² day ⁻¹
Hargrave et al. 1993	Bay of Fundy (E Canada)	TOU: 71–149 mmol O ₂ m ⁻² day ⁻¹
(Meijer and Avnimelech 1999)	Two ponds (Israel)	DOU: 70 mmol O ₂ m ⁻² day ⁻¹
Nickell et al. 2003	Loch Creran (W Scotland)	TOU: 295–575 mmol O ₂ m ⁻² d ⁻¹
Mulsow et al. 2006	Pillan and Reñihue Fjords (S Chile)	DOU: 152–1,200 mmol O ₂ m ⁻² day ⁻¹
This study	Loch Creran (W Scotland)	TOU: 23.2–67.9 mmol O ₂ m ⁻² day ⁻¹ DOU: 23.2–127.8 mmol O ₂ m ⁻² day ⁻¹

impacted site (Table 4), the DIC/O₂ ratio highlights the bimodality and variability within the vacated fish farm sediment. Indeed, this variation suggests a patchy distribution within the impacted station S5/S11 of predominant anaerobic (DIC/O₂ < 1) and oxic (DIC/O₂ > 1) mineralization processes.

In summary, the sediment below the vacated fish farm (at S5 and S11) was heterogeneous with two separate classes of sediments: intermediately impacted with DOU and TOU averaging 50 mmol O₂ m⁻² day⁻¹, DIC/O₂ ratio < 1, and the absence of sulphide in sediments, and highly impacted sediments with DOU averaging 100 mmol O₂ m⁻² day⁻¹ associated with black sulphidic sediments, DIC/O₂ ratio > 1 and H₂S gradients in pore-water in the first centimetre.

4.3 Differential Organic Matter Remineralization Activities in Loch Creran

Enhancement of organic matter degradation in sediments beneath fish farms has been widely documented (e.g. Hall et al. 1990; 1992); for a review, see Brooks and Mahnken (2003). It is worth mentioning that station S5 seems to display lower OC contents than S11: nevertheless, OC contents and C/N ratios are based on a single core measurement when planar optode images (Fig. 8) and microelectrode profiles (Fig. 5) clearly show a microscale heterogeneity. Based on their higher OC contents and DOU fluxes compared to S1 and their location within the fish farm vicinity, we coupled S5 and S11 and referred to them as S5/S11. The sharp transition at depth in the sediment OC content and lower C/N ratio profiles at S5/S11 (Fig. 3) clearly reflects the massive organic matter inputs from the fish farm. Such a transition does not exist at station S1: the average OC content at station S1 corresponds to the OC content found at depth in the sediment of the S5/S11 impacted stations. The high OC content in S5/S11 sediment is indicative of the organic enrichment that occurred in the recent past at the fish farm site, through high inputs of fish faeces and waste food.

This material is known to be very labile due to its high protein content (Kitagima and Fracalossi 2010) and is rapidly degraded by microbial respiration or eaten by mobile epifauna, which feed beneath active fish cages. The proteic nature of this material may explain the lower C/N ratio observed between 2- and 10-cm depth at station S11 (≈ 7–8 vs. 9–10, Fig. 3), which showed a large enrichment of organic matter in the top 8 cm (Nickell et al. 2003).

The current study began in March 2006, less than 3 months after the fish farming activity had ceased at this site and a proportion of the most labile organic components deposited in the sediment could have been removed. Still, during the 7 months of the

Table 6 Mass balance calculation for the carbon budget in the two sites of Loch Creran (in $\text{gC m}^{-2} \text{ year}^{-1}$)

	Recycling rate	Burial rate	Total POC flux	Recycling efficiency
Reference (S1)	88 ± 13	32 ± 16	119 ± 20	73 %
Impacted (S5/S11)	175 ± 118	/	$2665^{\text{a}}\text{--}3600^{\text{b}}$	$5^{\text{b}}\text{--}7^{\text{a}}$ %

^a Calculate from the OC deposition underneath the fish farm

^b Estimated from Brigolin et al. (2009)

present study, it was apparent that high oxygen demand of sediments beneath the vacated fish farm supported high rates of benthic metabolism and organic carbon degradation.

Recycling of organic matter was more intense in the impacted area (S5/S11) as indicated by larger DOU fluxes under the vacated fish farm than at the reference site S1. The highest fluxes ($97 \pm 19 \text{ mmol O}_2 \text{ m}^{-2} \text{ day}^{-1}$) observed at stations S11/S5 are consistent with previous studies of fish farm sediments (Table 5).

H_2S porewater profiles were also very different between the impacted and the non-impacted sediments, reflecting the difference in early diagenetic processes intensity between the two sites; for instance, due to the buffering capacity of reactive iron towards dissolved sulphides in sediments (Zhu et al. 2012; Giordani et al. 2008), the presence of sulphide close to the sediment–water interface is a nonlinear function of the OM recycling intensity (Middelburg and Levin 2009). Once the threshold is reached, sulphides are not confined to deeper sediment porewater but reach the oxic–anoxic boundary where they get re-oxidised directly by oxygen (Canfield et al. 1993b). According to our measurements, sulphide appearance close to the SWI only occurred within the impacted S5/S11 site when the DOU rate flux was above $100 \text{ mmol O}_2 \text{ m}^{-2} \text{ day}^{-1}$ (Fig. 7a). Indeed, during the September deployments (i.e. when H_2S profile was performed simultaneously with O_2), when the DOU flux was lower than $100 \text{ mmol O}_2 \text{ m}^{-2} \text{ day}^{-1}$ (mostly around $50 \text{ mmol O}_2 \text{ m}^{-2} \text{ day}^{-1}$, on average), sulphide was not recorded in the upper sedimentary column either in the impacted sediments or in the reference station (see Table 3).

We estimated mass balance for carbon in these sediments in order to assess recycling efficiency of the reference and impacted sites. The OM rain rate to the sediment at the vacated fish farm can be estimated by the predictive algorithm of Brooks (2001) which links the fish farm characteristics (cage volume and fish population density) to food supply and to the deposition of OM under the fish cages. Assuming a grow-out cycle of 24 months, a fish density of 10 kg m^{-3} in a 16-m-deep cage, and using the following relation (total volatile solid = $0.009 + 1.59 \text{ POC}$, Brooks 2001), the average deposition rate was estimated to be $2,665 \text{ gC m}^{-2} \text{ year}^{-1}$.

$$\left(\frac{10 \text{ kg fish} \cdot \text{m}^{-3} * \text{cages 16 m deep} * 0.094 \text{ kg TVS kg fish}^{-1}}{730 \text{ days}} - 0.009 \right) \frac{1}{1.59} * 365 \text{ days/years} = 2,665 \text{ g POC} \cdot \text{m}^{-2} \cdot \text{year}^{-1}.$$

This result is in the same order of magnitude than the value reported by Brigolin et al. (2009) for the deposition under the fish cages ($3,600 \text{ g C m}^{-2} \text{ year}^{-1}$) in the same area based on the statistics of fish food delivery. Assuming that the OC degradation rates are equal to our DIC fluxes, we combined these two deposition values and estimated the mineralization efficiency at the vacated fish farm site (see Table 6). In order to compare

those with the reference site (S1), we assessed a benthic carbon mass balance at S1 using accumulation rates of 1–2 mm year⁻¹ as reported for Loch Creran and Loch Etive in previous studies. These are standard accumulation rates for eutrophicated coastal zones (Moodley et al. 1998; Howe et al. 2001; Loh et al. 2002; Schmidt et al. 2007). We assume a dry bulk density of 2.65 g cm⁻³ (Brigolin et al. 2009) and use measured porosity values (Fig. 2), OC contents (Fig. 3) and these sedimentation rates to calculate OC accumulation rates (see Table 6).

Hence, the share of mineralization over the total deposition of organic matter (mineralization efficiencies in Table 6) is 73 % at the reference site (S1) and only 5–6 % at the impacted site (S5/S11). This difference between the two sites could be linked to the exclusion of large macrofauna and the shift to bacterial-driven benthic community in the more impacted sites (see next section). In addition, this difference reflects the different nature of diagenetic reactions regarding their oxic/anoxic nature (Pastor et al. 2011; Canfield et al. 1993a), the non-steady-state conditions in the fish farm sediment with OC accumulation over 2 years of exploitation and the relaxation evolution afterwards.

The turnover time as calculated by the inventory/recycling rate reaches 6.4 years with the values of the inventory calculated using 6.5 % OC over 8 cm of sediments and an average porosity of 0.85 (Figs. 2, 3). The estimated recovery time needed, and the shift in infauna community composition, underlines the necessity to assess exploitation modalities of fish farms in order to avoid a saturation of the system that would lead to hypoxia events (Dedieu et al. 2007) and consequently large changes in infauna habitats (Rowe et al. 2002; Kutti et al. 2007).

4.4 Impact on Loch Creran Benthic Ecosystems

General effects of organic loading from salmon farms on coastal benthic communities are well documented (Hargrave et al. 1993; Strain et al. 1995; Brooks 2001; Hall et al. 1990, 1992). Massive increase in abundance and biomass of OC tolerant opportunistic species generally occur in the fish farm site (Brooks et al. 2003, 2004; Brooks and Mahnken 2003; Kutti et al. 2007; Dupont et al. 2007). Samples from station S1 (e.g. cores and SPI/planar optode images), with well-oxygenated sediment, showed more evidence of numerous and deeper dwelling infauna, predominantly polychaete, than at the impacted S5/S11 site. Evidences of macrofaunal activity in S1 were also present in some planar optode images showing active burrows (Fig. 8c). On the contrary, macro and meiofauna seem excluded from the sediment under the vacated fish farm (S5/S11), as illustrated by a TOU/DOU ratio of 0.9. The difference in irrigation between the reference and impacted sites (TOU/DOU ratios of 1.7 and 0.9, respectively) matches the difference in bioturbation rates calculated for the same area by Nickell et al. (2003). They found a lower bioturbation rate by a factor of 5–6 in the zone impacted by the fish farm, as a consequence to the dominance in abundance and biomass of capitellid and dorvilleid polychaetes. These two species are well-known opportunists, capable of tolerating sulphide concentrations up to 7,200 $\mu\text{mol l}^{-1}$ (Hargrave et al. 1993, 1997). As a matter of fact, high concentrations of sulphides up to 1 mmol l⁻¹ at 3-cm depth were recorded in the porewater of the impacted stations (Fig. 7).

Heavy loading of organic matter by the fish farm clearly induced a change of the environment promoting anoxic conditions. Macrofaunal species non-tolerant to H₂S were excluded from these sediments and bacteria predominated. Relatively high bacterial abundances along with high sulphides concentrations were observed in October at station S5/S11 (Fig. 4). This is likely related to the growth of sulphate-reducing bacteria throughout the core (cf. Fig. 6). Indeed, at the same location, Nickell et al. (2003) noted a

thin and patchy, white, sulphide-oxidising bacterial mat on the fish farm sediment which they attributed to *Beggiatoa* spp., and similar observations were made by divers at station S5/S11 in October 2006.

Godbold and Solan (2009) reported the faunal assemblages along the enrichment gradient in Loch Creran at similar stations as ours. Species richness decreased from the reference to the impacted stations (S7 in their study is equivalent to our S11 site). The loss in species richness was associated with a change in assemblage composition from irrigators (e.g. *Mysella bidentata*) or tube dwelling/burrowing polychetes (e.g. *Melina Palmata*) to capitellid and dorvilleid species. The change of species richness can be related to a change in the bioturbation function (sediment mixed layer—ML) as a result of the enrichment gradient: indeed, a strong statistical relationship links OC content, species richness and ML. The processes behind this relationship are only hypothesized by Godbold and Solan (2009), and this study allows going one step further in the understanding of the ecosystem shift.

We report that, together with bioturbation, the irrigation function of the ecosystem as indicated by the TOU/DOU ratio was also largely diminished along the organic enrichment gradient. It is noteworthy that TOU/DOU represents the actual irrigation of the sediment compared to the potential irrigation as can be inferred from the faunal composition. We also report that changes in porewater composition, linked to organic matter diagenesis, influenced the ecosystem function. High sulphide concentrations in surface porewater are highly detrimental to the macrobenthic infauna and thus play a role in shaping the faunal assemblage and its bioturbation/irrigation capacity.

We can also make a scenario of the evolution from a reference sediment to an impacted sediment (Rosenberg et al. 2002). The large input of organic matter leads to the rapid reduction of the oxic layer to about 1 mm. Further accumulation of organic matter leads to stronger reduction of the oxic surface layer and the appearance of sulphide in organic hot spots of the sediment. When the limit of the buffering capacity of reactive iron towards dissolved sulphides in sediments has been reached (Zhu et al. 2012), sulphide concentrations begin to rise in porewater near the sediment–water interface pushing motile invertebrates upwards or out of the sediment and reducing bioturbation and irrigation (Peterson et al. 1996). This reduction further limits sulphide reoxidation, promoting H₂S to spread upward within the sedimentary column and this positive feedback continues until most sulphide-intolerant fauna is pushed out of the sediment.

Regarding the fate of sediments after the displacement of the fish cages away from its position, biological remediation of the site will probably involve colonisation by bigger and more diverse organisms as the sediment is re-oxidised and the microbial community evolve (Rhoads and Germano 1982, 1986; Pearson and Rosenberg 1978). Nevertheless, due to the degradation turnover time (about 6 years) and the lack of large irrigating fauna in the sediment, the timescale of recovery is largely uncertain.

5 Conclusions

Different in situ techniques were used to investigate the sediment organic matter cycling in a Scottish Loch impacted by fish farming. This multi-technique study describes the multi-scale benthic variability together with oxygen flux measurements. We showed a variability at the centimetre scale with benthic structures and organic hot spots, at the station scale below the fish farm with highly organic-loaded and moderately loaded sediments

underneath the vacated fish farm linked to the fish cages location, and at the Loch scale with a clear gradient between the reference station and the vacated fish farm sediments.

We provide further evidence of the fish farm impact on the sediment when compared to the reference background station. Large spots of organic rich, sulphidic black sediments were present below the vacated fish farm and exhibited large gradients in dissolved sulphide and extreme oxygen consumption. The large input of organic matter from the fish farm leads to a larger bacterial biomass and a shift from oxic–suboxic to anoxic diagenesis and induced a rapid shift in the sediment biogeochemical processes. The sulphidic nature of the fish farm sediments induces a change in ecosystem biota with smaller opportunistic species tolerant to sulphide (cappitellidae) replacing the larger more diverse fauna present in the reference stations. We showed that this creates a large change in irrigation activity as estimated by the TOU/DOU ratio which decreases from 1.7 in the reference zone to less than 1 in the impacted zone.

The residence time of the organic loading is about 6 years, but due to the lack of irrigation and the large presence of sulphide, resilience towards the initial state could be much longer. Such recovery timescales should be considered when setting up a legal framework to regulate fish farming activities.

Acknowledgments We would like to thank the invited editors of the special issue of Aquatic Geochemistry honouring the career of Bjorn Sundby for inviting us to write this paper. This work was part of the Specific Targeted Research Project (STREP) COBO (Coastal Ocean Benthic Observatory) sponsored by the European Union (contract no. 505564). We gratefully acknowledge the Captain and crew of RVs Calanus and Seol Mara from SAMS, and the assistance of the COBO group for operation at sea. H. Stahl provided the background data for Chl_a, oxygen and temperature. We also acknowledge support from Melanie Hartwich (Potsdam University, Germany) for bacteria counting and Graham Shimmield (coordinator of COBO) for general logistics at SAMS. R.N. Glud and H. Stahl provided additional 2-D O₂ images from another planar optode. We would like to thank the three anonymous reviewers who provided constructive comments that helped to improve our manuscript. This is LSCE contribution number 4849.

References

- Andrews D, Bennett A (1981) Measurements of diffusivity near the sediment-water interface with a fine-scale resistivity probe. *Geochim Cosmochim Acta* 45(11):2169–2175
- Apler A (2007) Effects of simulated natural and man-made resuspension on sediment-water exchange of oxygen and dissolved inorganic carbon—in situ studies in a Scottish sea loch. Master thesis, Göteborgs Universitet, Göteborg
- Avnimelech Y, Ritvo G, Meijer LE, Kochba M (2001) Water content, organic carbon and dry bulk density in flooded sediments. *Aquacult Eng* 25(1):25–33. doi:10.1016/s0144-8609(01)00068-1
- Barnett PRO, Watson J, Connelly D (1984) A multiple corer for taking virtually undisturbed samples from shelf, bathyal and abyssal sediments. *Oceanol Acta* 7(4):399–408
- Berg P, Risgaard-Petersen N, Rysgaard S (1998) Interpretation of measured concentration profiles in sediment pore water. *Limnol Oceanogr* 43(7):1500–1510
- Berner RA (1980) *Early Diagenesis: a theoretical approach*. Princeton Series in Geochemistry. Princeton University Press, Princeton
- Boudreau BP, Jørgensen BB (2001) *The benthic boundary layer—transport processes and biogeochemistry*. Oxford University Press, New York
- Brigolin D, Davydov A, Pastres R, Petrenko I (2008) Optimization of shellfish production carrying capacity at a farm scale. *Appl Math Comput* 204(2):532–540. doi:10.1016/j.amc.2008.05.118
- Brigolin D, Pastres R, Nickell TD, Cromey CJ, Aguilera DR, Regnier P (2009) Modelling the impact of aquaculture on early diagenetic processes in sea loch sediments. *Mar Ecol-Prog Ser* 388:63–80. doi:10.3354/meps08072
- Brooks KM (2001) An evaluation of the relationship between salmon farm biomass, organic inputs to sediments, physicochemical changes associated with those inputs and the infaunal response—with

- emphasis on Total Sediment Sulfides, Total Volatile Solids, and Oxydation-Reduction Potential as surrogate endpoints for biological monitoring. Available from Technical Advisory Group
- Brooks KM, Mahnken CVW (2003) Interactions of Atlantic salmon in the Pacific northwest environment II. Organic wastes. *Fish Res* 62(3):255–293
- Brooks KM, Stierns AR, Mahnken CVW, Blackburn DB (2003) Chemical and biological remediation of the benthos near Atlantic salmon farms. *Aquaculture* 219(1–4):355–377
- Brooks KM, Stierns AR, Backman C (2004) Seven year remediation study at the Carrie Bay Atlantic salmon (*Salmo salar*) farm in the Broughton Archipelago, British Columbia, Canada. *Aquaculture* 239(1–4): 81–123
- Canfield DE, Jørgensen BB, Fossing H, Glud R, Gundersen J, Ramsing NB, Thamdrup B, Hansen JW, Nielsen LP, Hall POJ (1993a) Pathways of organic carbon oxidation in three continental margin sediments. *Mar Geol* 113(1–2):27–40
- Canfield DE, Thamdrup B, Hansen JW (1993b) The anaerobic degradation of organic-matter in Danish coastal sediments—iron reduction, manganese reduction, and sulfate reduction. *Geochim Cosmochim Acta* 57(16):3867–3883
- Cathalot C, Rabouille C, Pastor L, Deflandre B, Viollier E, Buscail R, Gremare A, Treignier C, Pruski A (2010) Temporal variability of carbon recycling in coastal sediments influenced by rivers: assessing the impact of flood inputs in the Rhone River prodelta. *Biogeosciences* 7(3):1187–1205
- Chapelle A, Lazure P, Souchu P (2001) Modelling anoxia in the Thau lagoon (France). *Oceanol Acta* 24:S87–S97
- Dedieu K, Rabouille C, Thouzeau G, Jean F, Chauvaud L, Clavier J, Mesnage V, Ogier S (2007) Benthic O-2 distribution and dynamics in a Mediterranean lagoon (Thau, France): an in situ microelectrode study. *Estuar Coast Shelf Sci* 72(3):393–405
- Duport E, Gilbert F, Poggiale JC, Dedieu K, Rabouille C, Stora G (2007) Benthic macrofauna and sediment reworking quantification in contrasted environments in the Thau Lagoon. *Estuar Coast Shelf Sci* 72(3):522–533
- Edwards A, Sharples F (1985) Scottish sea lochs: a catalogue. SMBA Internal Report, vol 134
- Giordani G, Azzoni R, Viaroli P (2008) A rapid assessment of the sedimentary buffering capacity towards free sulphides. *Hydrobiologia* 611:55–66. doi:10.1007/s10750-008-9457-2
- Glud RN, Tengberg A, Kühl M, Hall POJ, Klimant I, Host G (2001) An in situ instrument for planar O-2 optode measurements at benthic interfaces. *Limnol Oceanogr* 46(8):2073–2080
- Glud RN, Wenzhofer F, Tengberg A, Middelboe M, Oguri K, Kitazato H (2005) Distribution of oxygen in surface sediments from central Sagami Bay, Japan: in situ measurements by microelectrodes and planar optodes. *Deep-Sea Res Part I Oceanogr Res Pap* 52(10):1974–1987
- Glud RN, Ståhl H, Berg P, Wenzhofer F, Oguri K, Kitazato H (2009) In situ microscale variation in distribution and consumption of O-2: a case study from a deep ocean margin sediment (Sagami Bay, Japan). *Limnol Oceanogr* 54(1):1–12
- Godbold JA, Solan M (2009) Relative importance of biodiversity and the abiotic environment in mediating an ecosystem process. *Mar Ecol-Prog Ser* 396:273–282. doi:10.3354/meps08401
- Grasshoff K, Ehrhardt M, Kremling K (1983) Methods of seawater analysis. Verlag Chemie
- Hall POJ, Anderson LG, Holby O, Kollberg S, Samuelsson MO (1990) Chemical fluxes and mass balances in a marine fish cage farm. 1. Carbon. *Mar Ecol-Prog Ser* 61 (1–2):61–73. doi:10.3354/meps061061
- Hall POJ, Holby O, Kollberg S, Samuelsson MO (1992) Chemical fluxes and mass balances in a marine fish cage farm. 4. Nitrogen. *Mar Ecol-Prog Ser* 89(1):81–91. doi:10.3354/meps089081
- Hansen K, Kristensen E (1997) Impact of macrofaunal recolonization on benthic metabolism and nutrient fluxes in a shallow marine sediment previously overgrown with macroalgal mats. *Estuar Coast Shelf Sci* 45(5):613–628
- Hargrave BT, Duplisea DE, Pfeiffer E, Wildish DJ (1993) Seasonal-Changes in benthic fluxes of dissolved-oxygen and ammonium associated with marine cultured Atlantic salmon. *Mar Ecol-Prog Ser* 96(3):249–257
- Hargrave BT, Phillips GA, Doucette LI, White MJ, Milligan TG, Wildish DJ, Cranston RE (1997) Assessing benthic impacts of organic enrichment from marine aquaculture. *Water Air Soil Pollut* 99(1–4): 641–650
- Hargrave BT, Doucette LI, Cranford PJ, Law BA, Milligan TG (2008) Influence of mussel aquaculture on sediment organic enrichment in a nutrient-rich coastal embayment. *Mar Ecol-Prog Ser* 365:137–149
- Hetland RD, DiMarco SF (2008) How does the character of oxygen demand control the structure of hypoxia on the Texas-Louisiana continental shelf? *J Mar Syst* 70(1–2):49–62. doi:10.1016/j.jmarsys.2007.03.002
- Howe JA, Stoker MS, Woolfe KJ (2001) Deep-marine seabed erosion and gravel lags in the northwestern Rockall Trough, North Atlantic Ocean. *J Geol Soc* 158:427–438

- Kitagima RE, Fracalossi DM (2010) Validation of a methodology for measuring nutrient digestibility and evaluation of commercial feeds for channel catfish. *Sci Agric* 67(5):611–615. doi:[10.1590/s0103-90162010000500016](https://doi.org/10.1590/s0103-90162010000500016)
- Kutti T, Hansen PK, Ervik A, Hoisaeter T, Johannessen P (2007) Effects of organic effluents from a salmon farm on a fjord system. II. Temporal and spatial patterns in infauna community composition. *Aquaculture* 262(2–4):355–366
- Lansard B, Rabouille C, Massias D (2003) Variability in benthic oxygen fluxes during the winter-spring transition in coastal sediments: an estimation by in situ micro-electrodes and laboratory mini-electrodes. *Oceanol Acta* 26(3):269–279
- Lansard B, Rabouille C, Denis L, Grenz C (2009) Benthic remineralization at the land-ocean interface: a case study of the Rhone River (NW Mediterranean Sea). *Estuar Coast Shelf Sci* 81(4):544–554. doi:[10.1016/j.ecss.2008.11.025](https://doi.org/10.1016/j.ecss.2008.11.025)
- Loh PS, Reeves AD, Overnell J, Harvey SM, Miller AEJ (2002) Assessment of terrigenous organic carbon input to the total organic carbon in sediments from Scottish transitional waters (sea lochs): methodology and preliminary results. *Hydrol Earth Syst Sci* 6(6):959–970
- Lu L, Wu RSS (1998) Recolonization and succession of marine macrobenthos in organic-enriched sediment deposited from fish farms. *Environ Pollut* 101(2):241–251
- Meijer LE, Avnimelech Y (1999) On the use of micro-electrodes in fish pond sediments. *Aquacult Eng* 21(2):71–83. doi:[10.1016/s0144-8609\(99\)00024-2](https://doi.org/10.1016/s0144-8609(99)00024-2)
- Middelboe M, Glud RN, Finster K (2003) Distribution of viruses and bacteria in relation to diagenetic activity in an estuarine sediment. *Limnol Oceanogr* 48(4):1447–1456
- Middelburg JJ, Levin LA (2009) Coastal hypoxia and sediment biogeochemistry. *Biogeosciences* 6(7):1273–1293
- Mienert J, Schultheiss PJ (1989) Physical properties of sedimentary environments in oceanic high (Site 658) and low (Site 659) productivity zones. Annotation: Woods Hole Oceanogr Inst, Contrib No 6796 108:397–406
- Moodley L, Heip CHR, Middelburg JJ (1998) Benthic activity in sediments of the northwestern Adriatic Sea: sediment oxygen consumption, macro- and meiofauna dynamics. *J Sea Res* 40(3–4):263–280
- Mulsow S, Krieger Y, Kennedy R (2006) Sediment profile imaging (SPI) and micro-electrode technologies in impact assessment studies: example from two fjords in Southern Chile used for fish farming. *J Mar Syst* 62(3–4):152–163
- Nickell LA, Black KD, Hughes DJ, Overnell J, Brand T, Nickell TD, Breuer E, Martyn Harvey S (2003) Bioturbation, sediment fluxes and benthic community structure around a salmon cage farm in Loch Creran, Scotland. *J Exp Mar Biol Ecol* 285–286:221–233. doi:[10.1016/s0022-0981\(02\)00529-4](https://doi.org/10.1016/s0022-0981(02)00529-4)
- Oconnor BDS, Costelloe J, Keegan BF, Rhoads DC (1989) The use of remots technology in monitoring coastal enrichment resulting from mariculture. *Mar Pollut Bull* 20(8):384–390
- Pamatmat MM, Bhagwat AM (1973) Anaerobic metabolism in Lake Washington sediments. *Limnol Oceanogr* 18(4):611–627
- Pastor L, Cathalot C, Deflandre B, Viollier E, Soetaert K, Meysman FJR, Ulses C, Metzger E, Rabouille C (2011) Modeling biogeochemical processes in sediments from the Rhone River delta area (NW Mediterranean Sea). *Biogeosciences* 8(5):1351–1366. doi:[10.5194/bg-8-1351-2011](https://doi.org/10.5194/bg-8-1351-2011)
- Pearson TH, Rosenberg R (1978) Macrobenthic succession in relation to organic enrichment and pollution of the marine environment. *Oceanogr Mar Biol Annu Rev* 16:229–311
- Peterson GS, Ankley GT, Leonard EN (1996) Effect of bioturbation on metal-sulfide oxidation in surficial freshwater sediments. *Environ Toxicol Chem* 15(12):2147–2155. doi:[10.1897/1551-5028\(1996\)015<2147:eoboms>2.3.co;2](https://doi.org/10.1897/1551-5028(1996)015<2147:eoboms>2.3.co;2)
- Pomeroy LR, Wiebe WJ (2001) Temperature and substrates as interactive limiting factors for marine heterotrophic bacteria. *Aquat Microb Ecol* 23(2):187–204. doi:[10.3354/ame023187](https://doi.org/10.3354/ame023187)
- Rabouille C, Denis L, Dedieu K, Stora G, Lansard B, Grenz C (2003) Oxygen demand in coastal marine sediments: comparing in situ microelectrodes and laboratory core incubations. *J Exp Mar Biol Ecol* 285:49–69
- Rabouille C, Conley DJ, Dai MH, Cai WJ, Chen CTA, Lansard B, Green R, Yin K, Harrison PJ, Dagg M, McKee B (2008) Comparison of hypoxia among four river-dominated ocean margins: the Changjiang (Yangtze), Mississippi, Pearl, and Rhone rivers. *Cont Shelf Res* 28(12):1527–1537. doi:[10.1016/j.csr.2008.01.020](https://doi.org/10.1016/j.csr.2008.01.020)
- Reimers CE, Smith KL (1986) Reconciling measured and predicted fluxes of oxygen across the deep-sea sediment-water interface. *Limnol Oceanogr* 31(2):305–318
- Revsbech NP (1989) An oxygen microsensor with a guard cathode. *Limnol Oceanogr* 34(2):474–478

- Rhoads DC, Germano JD (1982) Characterization of organism-sediment relations using sediment profile imaging—an efficient method of remote ecological monitoring of the seafloor (remotstm system). *Mar Ecol-Prog Ser* 8(2):115–128
- Rhoads DC, Germano JD (1986) Interpreting long-term changes in benthic community structure—a new protocol. *Hydrobiologia* 142:291–308
- Rosenberg R, Agrenius S, Hellman B, Nilsson HC, Norling K (2002) Recovery of marine benthic habitats and fauna in a Swedish fjord following improved oxygen conditions. *Mar Ecol-Prog Ser* 234:43–53
- Rowe GT, Kaegi MEC, Morse JW, Boland GS, Briones EGE (2002) Sediment community metabolism associated with continental shelf hypoxia, Northern Gulf of Mexico. *Estuaries* 25(6A):1097–1106
- Røy H, Huttel M, Jørgensen BB (2002) The role of small-scale sediment topography for oxygen flux across the diffusive boundary layer. *Limnol Oceanogr* 47(3):837–847
- Schmidt S, Jouanneau JM, Weber O, Lecroart P, Radakovitch O, Gilbert F, Jezequel D (2007) Sedimentary processes in the Thau Lagoon (France): from seasonal to century time scales. *Estuar Coast Shelf Sci* 72(3):534–542. doi:10.1016/j.ecss.2006.11.019
- Ståhl H (2001) Carbon cycling in deep-sea and contrasting continental margin sediments. PhD, Göteborg University, Göteborg
- Strain PM, Wildish DJ, Yeats PA (1995) The application of simple models of nutrient loading and oxygen demand to the management of a marine tidal inlet. *Mar Pollut Bull* 30(4):253–261
- Teal LR, Bulling MT, Parker ER, Solan M (2008) Global patterns of bioturbation intensity and mixed depth of marine soft sediments. *Aquatic Biol* 2(3):207–218. doi:10.3354/ab00052
- Tengberg A, De Bovee F, Hall P, Berelson W, Chadwick D, Ciceri G, Crassous P, Devol A, Emerson S, Gage J, Glud R, Graziottini F, Gundersen J, Hammond D, Helder W, Hinga K, Holby O, Jahnke R, Khripounoff A, Lieberman S, Nuppenau V, Pfannkuche O, Reimers C, Rowe G, Sahami A, Sayles F, Schurter M, Smallman D, Wehrli B, De Wilde P (1995) Benthic chamber and profiling landers in oceanography—a review of design, technical solutions and functioning. *Prog Oceanogr* 35:253–294
- Tengberg A, Ståhl H, Gust G, Muller V, Arning U, Andersson H, Hall POJ (2004) Intercalibration of benthic flux chambers I. Accuracy of flux measurements and influence of chamber hydrodynamics. *Prog Oceanogr* 60(1):1–28
- Ullman WJ, Aller RC (1982) Diffusion-coefficients in nearshore marine-sediments. *Limnol Oceanogr* 27(3):552–556
- Valiela I, Foreman K, Lamontagne M, Hersh D, Costa J, Peckol P, Demeoandreson B, Davanzo C, Babione M, Sham CH, Brawley J, Lajtha K (1992) Couplings of watersheds and coastal waters—sources and consequences of nutrient enrichment in Waquoit Bay, Massachusetts. *Estuaries* 15(4):443–457
- Vaquer-Sunyer R, Duarte CM (2010) Sulfide exposure accelerates hypoxia-driven mortality. *Limnol Oceanogr* 55(3):1075–1082
- Wenzhofer F, Glud RN (2004) Small-scale spatial and temporal variability in coastal benthic O₂ dynamics: effects of fauna activity. *Limnol Oceanogr* 49(5):1471–1481
- Zhu M-X, Liu J, Yang G-P, Li T, Yang R-J (2012) Reactive iron and its buffering capacity towards dissolved sulfide in sediments of Jiaozhou Bay, China. *Marine Environ Res* 80:46–55